Earth, Moon, and Planets (2006)
DOI 10.1007/s11038-006-9115-5

Geo-Neutrinos: from Theory to the KamLAND Results

GIOVANNI FIORENTINI
Dipartimento di Fisica, Università di Ferrara, I-44100, Ferrara, Italy
Istituto Nazionale di Fisica Nucleare, Sezione di Ferrara, I-44100, Ferrara, Italy

MARCELLO LISSIA
Istituto Nazionale di Fisica Nucleare, Sezione di Cagliari, I-09042, Monserrato (CA), Italy
Dipartimento di Fisica, Università di Cagliari, I-09042, Monserrato (CA), Italy

FABIO MANTOVANI
Dipartimento di Scienze della Terra, Università di Siena, I-53100, Siena, Italy
Centro di GeoTecnologie CGT, I-52027, San Giovanni Valdarno, Italy
Istituto Nazionale di Fisica Nucleare, Sezione di Ferrara, I-44100, Ferrara, Italy
(E-mail: fabio.mantovani@unisi.it)

BARBARA RICCI
Dipartimento di Fisica, Università di Ferrara, I-44100, Ferrara, Italy
Istituto Nazionale di Fisica Nucleare, Sezione di Ferrara, I-44100, Ferrara, Italy

(Received 1 March 2006; Accepted 19 July 2006)

Abstract. Earth shines in antineutrinos produced from long-lived radioactive elements: detection of this signal can provide a direct test of the Bulk Silicate Earth (BSE) model and fix the radiogenic contribution to the terrestrial heat flow. In this paper we present a systematic approach to geo-neutrino production based on global mass balance, supplemented by a detailed geochemical and geophysical study of the region near the detector, in order to build theoretical constraints on the expected signal. We show that the prediction is weakly dependent on mantle modeling while it requires a good description of the crust composition in the region of the detector site. In 2005 the KamLAND experiment proved that the technique for exploiting geo-neutrinos in the investigation of the Earth's interior is now available. After performing an analysis of KamLAND data which includes recent high precision measurements of the $^{13}C(\alpha, n)^{16}O$ cross section, we discuss the potential of future experiments for assessing the amount of uranium and thorium in different reservoirs (crust, mantle and core) of the Earth.

1. Introduction

The KamLAND collaboration has recently published (Araki et al., 2005) new experimental results, claiming some 28 geo-neutrino events from uranium and thorium decay chains in a two-year exposure. This important step shows that the technique for exploiting geo-neutrinos in the investigation of the Earth's interior is now available. In order to understand where to go with geo-neutrinos, we have to know where we stand in the light of the available data.

The most interesting feature of geo-neutrinos is that they bring to Earth's surface information coming from the entire planet concerning the amount of long-lived radioactive elements. Their detection, allowing for a quantitative determination of global elemental abundances, can provide a direct observational test of a classical geochemical paradigm, the Bulk Silicate Earth (BSE) model. Furthermore, geo-neutrinos can reveal the radiogenic contribution to terrestrial heat flow, providing thus an important contribution to the understanding of Earth's energetics.

In this review, mainly based on the results of our group (Fiorentini et al., 2005b; Mantovani et al., 2004; Fiorentini et al., 2005a; Fiorentini et al., 2003b; Fiorentini et al., 2003d), we shall address the following questions:

- What do we know about U, Th and ^{40}K in the Earth?
- What are the predictions and their uncertainties of a *reference* model for geo-neutrino production, i.e. of a model based on the current geochemical and geo-physical information?
- What is the contribution of the region near the detector? A close look at the nearby region is relevant in order to subtract from the geo-neutrino signal the local contribution, with the aim of determining the global component.
- How do we relate the geo-neutrino signal with the total mass of long-lived radioactive elements in the Earth?
- What are the implications of the KamLAND result?

Finally, we discuss the potential of future experiments for assessing the amounts of U and Th in different reservoirs (crust, mantle and core) of the Earth.

2. U, Th and K in the Earth: How much and where?

Earth's global composition is generally estimated from that of chondritic meteorites by using geochemical arguments which account for losses and fractionation during planet formation. Along these lines the Bulk Silicate Earth (BSE) model is built, which describes the "primitive mantle", i.e., the outer portion of the Earth after core separation and before the differentiation between crust and mantle. The model is believed to describe the present crust plus mantle system. Since lithophile elements should be absent in the core[1],

[1] One needs to be careful, since the definition of an element's behaviour, i.e., lithophile or not, depends on the surrounding system; there exist models of the Earth's core suggesting it is a repository for radioactive elements.

TABLE I
U, Th and K according to BSE, from (Fiorentini et al., 2003b)

	m [10^{17} kg]	H_R [10^{12} W]	L_v [10^{24} s^{-1}]
U	0.8	7.6	5.9
Th	3.1	8.5	5.0
^{40}K	0.8	3.3	21.6

the BSE provides the total amounts of U, Th and K in the Earth, estimates from different authors being concordant within 10–15% (McDonough, 2003). From the estimated masses, the present radiogenic heat production rate H_R and anti-neutrino luminosity L_v can be immediately calculated, see Table I and, e.g., (Fiorentini et al., 2005a).

The BSE is a fundamental geochemical paradigm. It is consistent with most observations, which regard mostly the crust and an undetermined portion of the mantle. The measurement of quantities – such as the geo-neutrino signals – which are directly related to the global amounts of radioactive elements in the Earth will provide a direct test of this model of the composition and origin of our planet.

Indeed, heat released from radiogenic elements is a major source of the terrestrial heat flow, however its role is not understood at a quantitative level. The masses estimated within the BSE account for a present radiogenic production of 19 TW, which is about one half of the estimated heat flow from Earth (McDonough, 2003, Hofmeister and Criss, 2005). Anderson refers (Anderson, 2005) to this difference as the missing heat source mystery and summarizes the situation with the following words: "Global heat flow estimates range from 30 to 44 TW ... Estimates of the radiogenic contribution ... based on cosmochemical considerations, vary from 19 to 31 TW. Thus, there is either a good balance between current input and output ... or there is a serious missing heat source problem, up to a deficit of 25 TW ..." If one can determine the amounts of radioactive elements by means of geo-neutrinos, an important ingredient of Earth's energetics will be fixed.

Concerning the distribution of radiogenic elements, estimates for uranium in the continental crust based on observational data are in the range:

$$m_C(U) = (0.3 - 0.4) \times 10^{17}\,\mathrm{kg} \tag{1}$$

The extreme values have been obtained in (Fiorentini et al., 2003b) by taking the lowest (highest) concentration reported in the literature for each layer of the Earth's crust, see Table II of (Mantovani et al., 2004), and integrating over a $2^\circ \times 2^\circ$ crust map. The main uncertainty comes from the uranium mass abundance a_{LC} in the lower crust, with estimates in the range (0.2–1.1) ppm. Estimates for the abundance in the upper crust, a_{UC}, are more concordant,

TABLE II
Average uranium abundance in the continental crust, from (Fiorentini et al., 2003b)

Reference	$\langle a_{CC} \rangle$ [ppm]
Taylor and McLennan, 1985	0.91
Weaver and Tarney, 1984	1.3
Rudnick and Fountain (1995)	1.42
Wedepohl (1995)	1.7
Shaw et al. (1986)	1.8
This work, minimal	1.3
This work, reference	1.54
This work, maximal	1.8

ranging from 2.2 to 2.8 ppm. The crust – really a tiny envelope – should thus contain about one half of the BSE prediction of uranium in the Earth.

About the mantle, observational data are scarce and restricted to the uppermost part, so the best estimate for its uranium content m_M is obtained by subtracting the crust contribution from the BSE estimate:

$$m_M = m_{BSE} - m_C \tag{2}$$

A commonly held view is that there is a vertical gradient in the abundances of incompatible elements in the mantle, with the top being most depleted. A minimum gradient model has a fully mixed and globally homogeneous mantle; the other extreme is a model where all the uranium is at the bottom of the mantle.

Geochemical arguments are against the presence of radioactive elements in the completely unexplored core, as discussed by McDonough in a recent review of compositional models of the Earth (McDonough, 2003).

Similar considerations hold for thorium and potassium, the relative mass abundance with respect to uranium being globally estimated as:

$$a(\mathrm{Th}) : a(\mathrm{U}) : a(\mathrm{K}) \approx 4 : 1 : 10,000 \tag{3}$$

We remark that the well-fixed ratios[2] in Eq. (3) imply that detection of geo-neutrinos from uranium will also bring important information on the amount of thorium and potassium in the whole Earth.

[2] We shall always refer to element abundances in mass and we remind the reader that the natural isotopic composition is $^{238}\mathrm{U/U} = 0.993$, $^{232}\mathrm{Th/Th} = 1$ and $^{40}\mathrm{K/K} = 1.2 \times 10^{-4}$.

3. A reference model and its uncertainties

3.1. Uranium, thorium and potassium distribution

Our aim is to build a reference model (labeled as "ref."), which incorporates the best available knowledge of U, Th and K distributions inside Earth. Concerning Earth's crust, we distinguish oceans and seawater, the continental crust, subdivided into three sublayers (upper, middle, and lower), sediments and oceanic crust. These seven layers have been mapped in (Bassin et al., 2000), which provides values of density and depth over the globe on a grid with 2° steps. We distinguish then the upper mantle (extending down to about 600 km), the lower mantle (down to about 2900 km), and the core: we use the preliminary reference earth model (PREM) (Dziewonski and Anderson, 1981) for the values of the densities of the mantle, assuming spherical symmetry.

For each component, one has to adopt a value for the abundances a(U), a(Th), and a(K). In the literature of the last twenty years one can find many estimates of abundances for the various components of the crust (OC, upper CC, lower CC,...), generally without an error value (see Tables II–IV of Mantovani et al., 2004), two classical reviews being in Refs. (Taylor and McLennan, 1985; Wedepohl, 1995) and a most useful source being provided by the GERM Reservoir Database (GERM, 2003).

For the upper mantle we are aware of several estimates by Jochum et al. (1986), White (1993), O'Nions and McKenzie (1993), Hofmann (1988), and Zartman and Haines (1988). In this respect data obtained from material emerged from unknown depths are assumed to be representative of the average composition down to about 600 km.

For each (sub)layer of the crust and for the upper mantle, we adopt as reference value for the uranium abundance $a^{\mathrm{ref}}(\mathrm{U})$ the average of the values reported in Tables II, III, and IV of (Mantovani et al., 2004). Concerning Th and K, we observe that the abundance ratios with respect to uranium are much more consistent among different authors than the corresponding absolute abundances. We shall thus take the average of ratios and from these construct the reference abundances for thorium and potassium:

$$a^{\mathrm{ref}}(\mathrm{Th}) = \langle \mathrm{Th}/\mathrm{U} \rangle a^{\mathrm{ref}}(\mathrm{U}) \quad \text{and} \quad a^{\mathrm{ref}}(\mathrm{K}) = \langle \mathrm{K}/\mathrm{U} \rangle a^{\mathrm{ref}}(\mathrm{U}) \tag{4}$$

For the lower mantle, where no observational data are available, we resort to the BSE model, which – we recall – describes the present crust-plus-mantle system based on geochemical arguments.

The mass of each element (X = U, Th, K) in the lower mantle $m_{\mathrm{LM}}(\mathrm{X})$ is thus obtained by subtracting from the BSE estimate the mass calculated for the crust and upper mantle:

TABLE III

Total yields. N_{no} is the total number of geoevents (U + Th) in the absence of oscillations predicted from the reference model for 10^{32} proton yr (or in TNU) and $\Delta N_{\rm no}$ is the "1σ" error

Location	$N_{\rm no}$	$\Delta N_{\rm no}$	$N_{\rm no}^{\rm low}$	$N_{\rm no}^{\rm high}$
Baksan	91	13	51	131
Hawaii	22	6	10	49
Homestake	91	13	51	130
Kamioka	61	10	33	96
Gran Sasso	71	11	39	106
Pyhasalmi	92	13	51	131
Sudbury	87	13	48	125
Curacao	57	10	30	92

$N_{\rm no}^{\rm low}$ ($N_{\rm no}^{\rm high}$) is the minimal (maximal) prediction. For $\delta m^2 > 4 \times 10^{-5}{\rm eV}^2$ the geoevent yield is $N = N_{\rm no}\left[1 - 0.5\sin^2(2\theta)\right]$, from (Mantovani et al., 2004).

TABLE IV

Errors from the regional geophysical and geochemical uncertainties at Kamioka, from (Fiorentini et al., 2005b)

Source	ΔS[TNU]	Remarks
Composition of upper-crust samples	0.96	3σ error
Upper-crust discretization	1.68	
Lower-crust composition	0.82	Full range
Crustal depths	0.72	3σ error
Subducting slab	2.10	Full range
Japan Sea	0.31	Full range
Total	3.07	Full range

$$m_{\rm LM}({\rm X}) = m_{\rm BSE}({\rm X}) - m_{\rm CC}({\rm X}) - m_{\rm OC}({\rm X}) - m_{\rm UM}({\rm X}) \tag{5}$$

Reference abundances for the lower mantle are then obtained by dividing these values by its mass $m_{\rm LM} = 2.9 \times 10^{24}$ kg. According to geochemical arguments, negligible amounts of U, Th and K should be present in the core. The resulting choice of input values for the reference model is collected in Tables II–IV of (Mantovani et al., 2004).

3.2. The uncertainties of the reference model

Since the abundance ratios look relatively well determined, we concentrate on the uncertainties of the uranium abundances in the different layers and

propagate them to the other elements. For the reference model, we have $m_{CC}(U) = 0.345 \times 10^{17}$ kg, $m_{OC}(U) = 0.005 \times 10^{17}$ kg, the total mass of CC being $m_{CC} = 2.234 \times 10^{22}$ kg. According to our model, the average uranium abundance in the CC is thus $a_{CC}(U) = 1.54 \times 10^{-6}$.

We determine a range of acceptable values of $a_{CC}(U)$ by taking the lowest (highest) concentration reported in the literature for each layer, see Table II of (Mantovani et al., 2004). The main source of uncertainty is from the abundance in the lower crust, estimated at 0.20 ppm in (Rudnick and Fountain, 1995) and at 1.1 ppm in (Shaw et al., 1986). Estimates for the abundance in the upper crust are more concordant, ranging from 2.2 ppm (Condie, 1993) to 2.8 ppm (Taylor and McLennan, 1985). We remark that, within this approach, the resulting average crustal U abundance $\langle a_{CC} \rangle$ is in the range 1.3–1.8 ppm, which encompasses all estimates reported in the literature (Rudnick and Fountain, 1995; Shaw et al., 1986; Wedepohl, 1995; Weaver and Tarney, 1984) except for that of (Taylor and McLennan, 1985), $\langle a_{CC} \rangle = 0.91$ ppm, see Table II.[3]

$$\text{low} : a_{CC}(U) = 1.3 \times 10^{-6}; a_{CC}(Th) = 5.2 \times 10^{-6}; a_{CC}(K) = 1.3 \times 10^{-2}$$

$$\text{high} : a_{CC}(U) = 1.8 \times 10^{-6}; a_{CC}(Th) = 7.6 \times 10^{-6}; a_{CC}(K) = 1.97 \times 10^{-2}$$

For the upper mantle, we take as extrema the two values known to us (Jochum et al., 1986; Zartman and Haines, 1988) for uranium and we deduce thorium and potassium by rescaling

$$\text{low} : a_{UM}(U) = 5 \times 10^{-9}; a_{UM}(Th) = 13 \times 10^{-9}; a_{UM}(K) = 6 \times 10^{-5}$$

$$\text{high} : a_{UM}(U) = 8 \times 10^{-9}; a_{UM}(Th) = 21 \times 10^{-9}; a_{UM}(K) = 9.6 \times 10^{-5}$$

Concerning the lower mantle, we fix the mass of radiogenic elements by requiring that the BSE constraint (3.2) is satisfied and we assume uniform abundance.

3.3. Predicted yields

The no oscillation yields, calculated with the fluxes of the reference model, are shown in Table XII of (Mantovani et al., 2004). In the same table we also present the estimated 1σ errors. The geo-neutrino signal is expressed in

[3] Note that this paper quotes ranges of mass and fluxes tighter than in (Mantovani et al., 2004), which used the value $\langle a_{CC} \rangle = 0.91$ ppm from (Taylor and McLennan, 1985) as lower limit.

Terrestrial Neutrino Units, one TNU corresponding to 10^{-32} geo-neutrino captures per target proton per year.

For the Kamioka site the prediction of the reference model is $N_{no} = 61$ TNU in good agreement with the "best model" of (Fiorentini et al., 2003a; Fiorentini et al., 2003c), $N_{no} = 67$ TNU, in between the values of (Rothschild et al., 1998), $N_{no} = 43$ TNU, and of model 1b of (Raghavan et al., 1998), $N_{no} = 75$ TNU.

4. A closer look for Kamioka

The geo-neutrino signal depends on the total uranium mass of radioactive elements in the Earth and on the geochemical and geophysical properties of the region around the detector (Fiorentini et al., 2003a). For KamLAND, we estimated (Mantovani et al., 2004) that about one half of the signal originates within 200 km from the detector. This region, although containing a globally negligible amount of uranium and thorium, produces a large contribution to the signal as a consequence of its proximity to the detector. This contribution has to be determined on the grounds of a detailed geochemical and geophysical study of the region, if one wants to extract from the total signal the remaining part which carries the relevant information. The study of the region around Kamioka, including the possible effects of the subducting plates below the Japan Arc and a discussion of the contribution from of the Japan Sea, is in (Fiorentini et al., 2005b).

Starting from the $2^\circ \times 2^\circ$ world crustal map, we isolated six "tiles", around Kamioka and we performed a detailed study of their uranium content, see Figure 1. The seismic velocity structure of the crust beneath the Japan Islands has been determined in (Zhao et al., 1992) from the study of some 13,000 arrival times of 562 local shallow earthquakes. By applying an inversion method, the depth distribution of the Conrad and Moho discontinuities beneath the whole of the Japan Islands are derived, with an estimated standard error of $\pm$ 1 km over most of Japan territory. This allows distinguishing two layers in the crust: an upper crust extending down to the Conrad and a lower part down to the Moho discontinuity.

The upper-crust chemical composition of Japan Islands has been studied in (Togashi et al., 2000), based on 166 representative specimens, which can be associated with 37 geological groups based on age, lithology and province. By combining the base geological map of Figure 2 of (Togashi et al., 2000) – which distinguishes 10 geological classes – with the abundances reported in Table I of the same paper, one can build a map of uranium abundance in the upper crust, under the important assumption that the composition of the whole upper crust is the same as that inferred in (Togashi et al., 2000) from the study of the exposed portion.

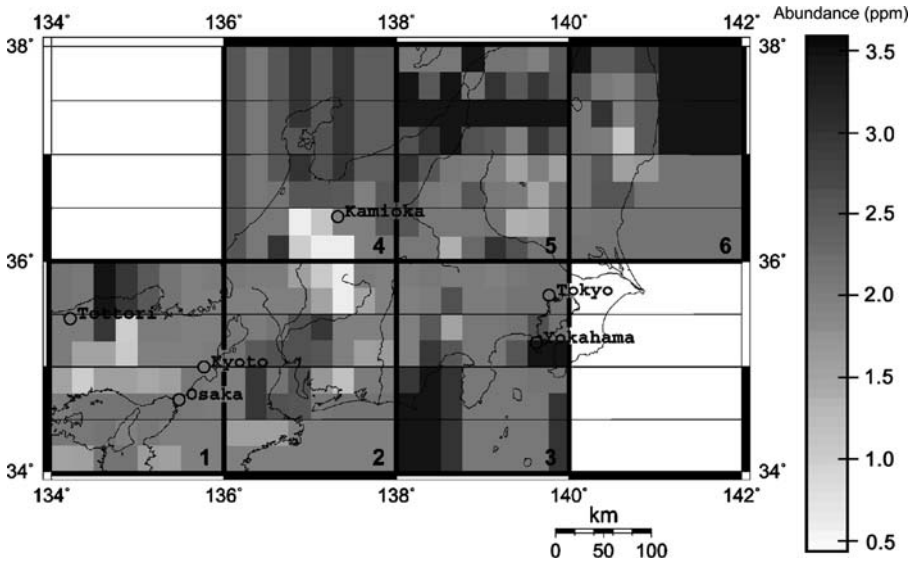

Figure 1. Uranium abundance in the upper crust of Japan (Fiorentini et al., 2005b).

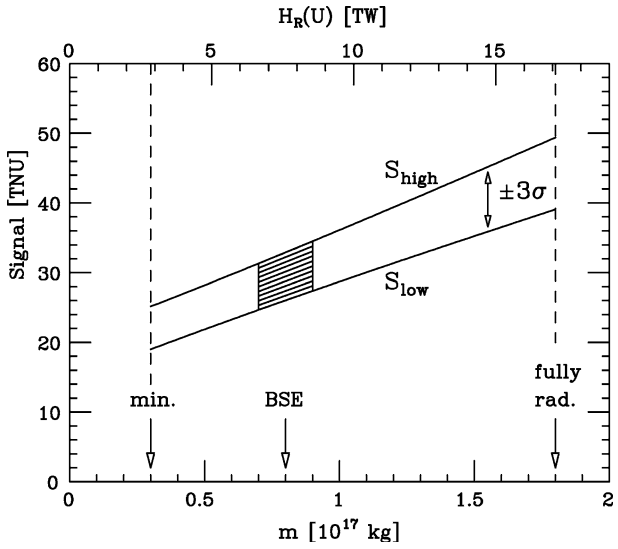

Figure 2. The predicted signal from uranium geo-neutrinos at KamLAND (Fiorentini et al., 2005b).

We are not aware of a specific study of the lower part of the Japan crust, however, it is well known that there are similarities between the composition of the Japanese crust and that of the Sino-Korean block. In an extensive compositional study of East China crust (Gao et al., 1998), the estimated uranium abundance in the lower part is between 0.63 and

1.08 ppm. On these grounds we shall take for the abundance in the lower crust of Japan:

$$a_{LC} = 0.85 \pm 0.23 \quad \text{ppm}$$

For the this discussion, we use the asymptotic value of the survival probability and the best fit value of the mixing angle, i.e. $\langle P_{ee} \rangle = 0.59$.[4]

The contributions to the produced flux and to the signal from the six tiles near Kamioka are:

$$\Phi_6 = 1.59 \times 10^6 \quad \text{cm}^{-2}\ \text{s}^{-1}$$

$$S_6 = 12.74 \quad \text{TNU}$$

With respect to our previous estimate from the whole globe (Mantovani et al., 2004), giving $\Phi = 3.676 \times 10^6\ \text{cm}^{-2}\text{s}^{-1}$ and $S = 28.6$ TNU, we find that the six tiles contribute 43% of the flux and 45% of the signal: this justifies the close scrutiny of the region within the six tiles. Some 3/4 of the contribution arises from the upper crust.

In more detail, the tile hosting Kamioka generates 29% and 30% of the total produced flux and signal, respectively. The host cell, i.e., the cell where Kamioka is located, contributes 9% to the total produced flux.

The uranium mass contained in the six tiles is about $m_6 = 3.3 \times 10^{13}$ kg, really negligible (less then 0.05%) with respect to that estimated for the whole Earth. We have considered several sources of the uncertainties affecting this estimate of the local contribution, see Table IV.

5. The geo-neutrino signal as a function of uranium mass in the Earth

The arguments presented in the previous sections permit a test of the BSE model, which fixes the total amount of long-lived radiogenic elements in the Earth. One can go further, and ask for a general relationship between the geo-neutrino signal and the total mass of uranium (and other radiogenic elements) in the Earth.

The main ingredient is what we call ''the proximity argument'', i.e. the fact that for a fixed mass the maximal (minimal) signal is obtained by placing the sources as close to (as far from) the detector as possible. We already isolated the contribution from the region near the detector and thus we concentrate on the contribution from different reservoirs in the rest of the world (RW), by

[4] For more details of the dependence of the survival probability on the distance with δm^2 (see Mantovani et al., 2004); the discussion of the errors on the oscillation parameters can be found at the end of section 5.4.

TABLE V
Minimal and maximal estimated uranium abundances for the continental crust in ppm, from (Fiorentini et al., 2005b)

	Min	Max
Upper crust	2.2	2.8
Lower crust	0.2	1.1

supplementing the proximity argument with the constraint that the distribution of radiogenic elements are consistent with geochemical and geophysical information on the globe.

5.1. The crusts contribution

For the Earth's crust, we use again the $2° \times 2°$ map of (Bassin et al., 2000) distinguishing several crustal layers which are known to contain different amounts of radioactive elements. For each layer minimal and maximal estimates of uranium abundances found in the literature are adopted, so as to obtain a range of acceptable fluxes, see Table V.

Depending on the adopted values, the uranium mass[5] in the crust $m_C(U)$ is in the range (0.3–0.4) in units – here and in the following – of 10^{17} kg. Clearly a larger mass means a bigger signal, the extreme values being:

$$S_C^{(min)}(U) = 6.448 \quad \text{TNU} \quad \text{for} \quad m_C(U) = 0.3 \quad \text{and}$$
$$S_C^{(max)}(U) = 8.652 \quad \text{TNU} \quad \text{for} \quad m_C(U) = 0.4$$

5.2. The contribution from the mantle

Concerning uranium in the mantle, we assume spherical symmetry and that the uranium mass abundance is a non-decreasing function of depth. It follows that, for a fixed uranium mass in the mantle $m_M(U)$, the extreme predictions for the signal are obtained by:

(i) placing uranium in a thin layer at the bottom and
(ii) distributing it with uniform abundance in the mantle.

[5] We are discussing uranium, however similar considerations hold for thorium.

These two cases give, respectively:

$$S_{\mathrm{M}}^{(\min)}(\mathrm{U}) = 12.15 \times m_{\mathrm{M}}(\mathrm{U}) \quad \mathrm{TNU} \quad \text{and}$$
$$S_{\mathrm{M}}^{(\max)}(\mathrm{U}) = 17.37 \times m_{\mathrm{M}}(\mathrm{U}) \quad \mathrm{TNU}$$

5.3. Crust and mantle

By using again the proximity argument, we can combine the contributions from crust and mantle so as to obtain extreme predictions: for a fixed total $m(\mathrm{U}) = m_{\mathrm{C}}(\mathrm{U}) + m_{\mathrm{M}}(\mathrm{U})$, the highest signal is obtained by assigning to the crust as much material as consistent with observational data ($m_{\mathrm{C}}(\mathrm{U}) = 0.4$) and putting the rest, $m(\mathrm{U}) - m_{\mathrm{C}}(\mathrm{U})$, in the mantle with a uniform distribution. Similarly, the minimal flux/signal is obtained for the minimal mass in the crust ($m_{\mathrm{C}}(\mathrm{U}) = 0.3$) and the rest in a thin layer at the bottom of the mantle. In conclusion, the contribution from the rest of the world is within the range:

$$S_{\mathrm{RW}}^{(\min)} = [6.448 + 12.15(m - 0.3)] \quad \mathrm{TNU} \text{ and}$$
$$S_{\mathrm{RW}}^{(\max)} = [8.652 + 17.37(m - 0.4)] \quad \mathrm{TNU}$$

5.4. Geo-neutrino signal and uranium mass

By combining the regional contribution, we get the uranium geo-neutrino signal as a function of uranium mass in the Earth:

$$S(\mathrm{U}) = S_0(\mathrm{U}) \pm \Delta(\mathrm{U})$$

where

$$S_0(\mathrm{U}) = 17.66 + 14.76 \times m(\mathrm{U})$$

and

$$\Delta^2(\mathrm{U}) = (3.07)^2 + [2.61 \times m(\mathrm{U}) - 0.55]^2 \tag{6}$$

This error is obtained by combining in quadrature all geochemical and geophysical uncertainties discussed in the preceding paragraphs. All of them have been estimated so as to cover $\pm 3\sigma$ intervals of experimental measurements and total ranges of theoretical predictions.

However, this error does not account for present uncertainties on neutrino oscillation parameters and on the cross section of the scattering

TABLE VI

Effect of the oscillation parameters on the signal. The relative/absolute variation is computed with respect to the prediction for the best fit values ($\delta m^2 = 7.9 \times 10^{-5}$ eV^2 and $\tan^2\theta = 0.40$), from (Fiorentini et al., 2005b)

Parameter	Signal variation
$\tan^2\theta = 0.26$	+13.5%
$\tan^2\theta = 0.67$	−12.2%
$\delta m^2 = 6.9 \times 10^{-5}$ eV^2	+0.11 TNU
$\delta m^2 = 9.3 \times 10^{-5}$ eV^2	−0.10 TNU

antineutrino-proton. For the sake of discussing the potential of geo-neutrinos, we shall ignore for the moment these error sources.

The expected signal from uranium geo-neutrinos at KamLAND is presented as a function of the total uranium mass m(U) in Figure 2. The upper horizontal scale indicates the corresponding radiogenic heat production rate from uranium ($H_R = 9.5 \times m$).

The predicted signal as a function of m(U) is between the two lines denoted as S_{high} and S_{low}, which correspond, respectively, to $S_0 \pm \Delta$.

Since the minimal amount of uranium in the Earth is 0.3×10^{17} kg (corresponding to the minimal estimate for the crust and the assumption of negligible amount in the mantle), we expect a signal of at least 19 TNU. On the other hand, the maximal amount of uranium tolerated by Earth's energetics[6], 1.8×10^{17} kg, implies a signal not exceeding 49 TNU.

For the central value of the BSE model, $m(U) = 0.8 \times 10^{17}$ kg, we predict $S(U) = 29.5 \pm 3.4$ TNU, i.e., with an accuracy of 12% at "3σ". We remark that estimates by different authors for the uranium mass within the BSE are all between $(0.7–0.9) \times 10^{17}$ kg. This implies that the uranium signal has to be in the interval (24.7–34.5) TNU. The measurement of geo-neutrinos can thus provide a direct test of an important geochemical paradigm.

The effect of uncertainties about the oscillation parameters is presented in Table VI. In this respect the mixing angle is most important. Figure 4 (b) of (Araki et al., 2005) shows a 3σ range $0.26 < \tan^2\theta < 0.67$ (central value 0.40): the corresponding range for the average survival probability is $0.52 < P_{ee} < 0.67$ (central value 0.59), with a 3σ relative error on the signal $\Delta S/S \approx 13\%$, which is comparable to the geological uncertainty in Eq. (5.1). The mixing angle should be determined more precisely for fully exploiting the geo-neutrino signal.

[6] For an uranium mass $m = 1.8 \times 10^{17}$ kg and relative abundances as in Eq. (3), the present radiogenic heat production rate from U, Th and K decays equals the maximal estimate for the present heat flow from Earth, $H_E^{max} = 44$ TW (Pollack et al., 1993).

5.5. Extension to thorium

The same analysis was extended to thorium in (Mantovani et al., 2004) assuming global chondritic uranium-to-thorium mass ratio, $m(\mathrm{Th})/m(\mathrm{U}) = 3.9 \pm 0.1$, so that we can now connect the combined signal at Kamioka due to geo-neutrinos from uranium and thorium progenies, S(U + Th), with the radiogenic heat production rate from these elements, H(U + Th), see Figure 3.

The allowed band in Figure 3 is estimated by considering rather extreme models for the distributions of radioactive elements, chosen so as to maximize or minimize the signal for a given heat production rate, see (Fiorentini et al., 2005b).

We also remark that, in comparison with the present experimental error, the width of the band is so narrow that we can limit the discussion to the median line of the allowed band in Figure 3, which represents our best estimate for the relationship between signal and radiogenic power.

By using the Bulk Silicate Earth (BSE) model, giving $H(\mathrm{U} + \mathrm{Th}) = 16$ TW, our prediction for Kamioka is centered at 37 TNU.

By assuming that uranium and potassium in the Earth are in the ratio 1/10,000 and that there is no potassium in the core, the total radiogenic power is $H(\mathrm{U} + \mathrm{Th} + \mathrm{K}) = 1.18\, H(\mathrm{U} + \mathrm{Th})$. With these assumptions, a maximal and fully radiogenic heat production rate, $H(\mathrm{U} + \mathrm{Th} + \mathrm{K}) = 44$ TW, corresponds to $H(\mathrm{U} + \mathrm{Th}) = 37$ TW, which gives signal $S(\mathrm{U} + \mathrm{Th}) \approx 56$ TNU.

6. Discussion of the KamLAND results

The KamLAND collaboration has reported (Araki et al., 2005) data from an exposure of $N_\mathrm{p} = (0.346 \pm 0.017) \times 10^{32}$ free protons over time $T = 749$ days with detection efficiency $\varepsilon = 69\%$: the effective exposure is thus $E_\mathrm{eff} = N_\mathrm{p} \times T \times \varepsilon = (0.487 \pm 0.025)\ 10^{32}$ protons· year. In the energy region where geo-neutrinos are expected, there are $C = 152$ counts, implying statistical fluctuation of ± 12.5. Of these counts, number $R = 80.4 \pm 7.2$ are attributed to reactor events, based on an independent analysis of higher energy data. Fake geo-neutrino events, originating from $^{13}\mathrm{C}(\alpha, \mathrm{n})^{16}\mathrm{O}$ reactions following the alpha decay of contaminant $^{210}\mathrm{Po}$, are estimated to be $F = 42 \pm 11$, where the error is due to 20% uncertainty on the $^{13}\mathrm{C}(\alpha, \mathrm{n})^{16}\mathrm{O}$ cross section and 14% uncertainty on the number of $^{210}\mathrm{Po}$ decays in the detector. Other minor backgrounds account for $B = 4.6 \pm 0.2$ events. The number of geo-neutrino events is estimated by subtraction, $N(\mathrm{U} + \mathrm{Th}) = C - R - F - B$, with an uncertainty obtained by combining the independent errors: $N(\mathrm{U} + \mathrm{Th}) = 25^{+19}_{-18}$. The geo-neutrino signal is thus

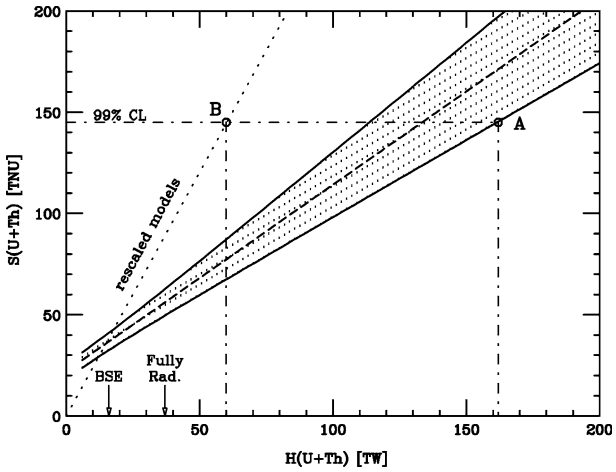

Figure 3. Predictions on the combined signal S(U + Th) from uranium and thorium geo-neutrinos at Kamioka as a function of the radiogenic heat production rate H(U + Th). The shaded area denotes the region allowed by geochemical and geophysical constraints. The dashed median line represents our best estimate for the relationship between signal and radiogenic power (Fiorentini et al., 2005a).

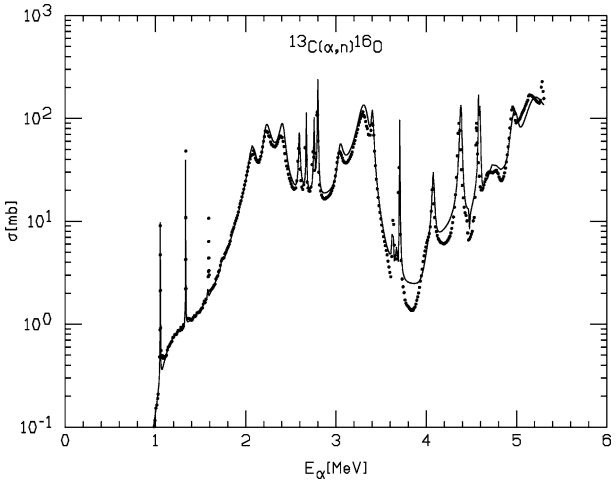

Figure 4. Cross section of $^{13}C(\alpha, n)^{16}O$. The solid line corresponds to the JENDL compilation, dots are the experimental points from (Harissopulos et al., 2005).

$S(\mathrm{U+Th}) = N(\mathrm{U+Th})/E_{\mathrm{eff}} = 51^{+39}_{-36}$ TNU. From the median line in Figure 3 one finds

$$H(\mathrm{U+Th}) = 31^{+43}_{-31}\mathrm{TW} \quad \text{(rate only)}$$

This "rate only" study has been improved in (Araki et al., 2005) by exploiting the shape of the spectrum. A likelihood analysis of the unbinned

spectrum yields $N(\mathrm{U}+\mathrm{Th}) = 28^{+16}_{-15}$, see Figure 4b of (Araki et al., 2005). This implies $S(\mathrm{U}+\mathrm{Th}) = 57^{+33}_{-31}$ TNU and

$$H(\mathrm{U}+\mathrm{Th}) = 38^{+35}_{-33}\mathrm{TW} \quad (\mathrm{rate} + \mathrm{spectrum})$$

The best fit value is close to the maximal and fully radiogenic model, however the BSE is within 1σ.

By using the median line in Figure 3, the 99% confidence limit on the signal (145 TNU) corresponds to 133 TW. If we include the uncertainty band of the theoretical models, we find an upper bound of 162 TW, see point in Figure 3. This point corresponds to a model with total uranium mass $m(\mathrm{U}) = 80 \times 10^{16}$ kg, an uranium poor crust, $m_c(\mathrm{U}) = 3 \times 10^{16}$ kg, the rest of the uranium being placed at the bottom of the mantle, and global chondritic thorium-to-uranium ratio.

This 162 TW upper bound is much higher than the 60 TW upper bound claimed in (Araki et al., 2005), which was obtained by using a family of geological models which are too narrow and are also incompatible with well-known geochemical and geophysical data, see (Fiorentini et al., 2005a).

We remark that the bound $H(\mathrm{U}+\mathrm{Th}) < 162$ TW which we have extracted from KamLAND data does not add any significant information on Earth's interior, since anything exceeding $H(\mathrm{U}+\mathrm{Th}) = 37$ TW [i.e. $H(\mathrm{U}+\mathrm{Th}+\mathrm{K}) = 44$ TW] is unrealistic. The upper limit simply reflects the large uncertainty in this pioneering experiment.

On the other hand, what is important for deciding the potential of future experiments is the relationship between geo-neutrino signal and heat production in the physically interesting region, $H(\mathrm{U}+\mathrm{Th}) \leq 37$ TW. The basic parameter is the slope, dS/dH, which expresses how the experimental error translates into an uncertainty on the deduced heat production. For our models we find from Figure 3 $dS/dH \sim 1$ TNU/TW. This slope is the same at any location. Discrimination between BSE and fully radiogenic models, which demands precision $\Delta H \sim 7$ TW, requires thus an experiment with an accuracy $\Delta S \sim 7$ TNU.

7. The geo-neutrino signal and the $^{13}\mathrm{C}(\alpha, \mathrm{n})^{16}\mathrm{O}$ cross section

As already remarked, a major uncertainty for extracting the geo-neutrino signal originates from the $^{13}\mathrm{C}(\alpha, \mathrm{n})^{16}\mathrm{O}$ cross section. The values used in (Araki et al., 2005) are taken from the JENDL (2005) compilation, which provides an *R*-matrix fit of relatively old data. A 20% overall uncertainty has been adopted in (Araki et al., 2005), corresponding to the accuracy claimed in the original experimental papers, see e.g. (Bair and Haas, 1973).

Recently, a series of high precision measurements for this cross section has been performed (Harissopulos et al., 2005). In the relevant energy range

$(1.0 \div 5.3)$ MeV, the absolute normalization has been determined within 4% accuracy. The measured values are generally in very good agreement with those recommended in JENDL, see Figure 4; however, we find that the neutron yield per alpha particle is 5% smaller. It follows that the number of fake neutrinos is lower, $F = 40 \pm 5.8$, and geo-neutrino events obviously increase.

The "rate only" analysis gives now 27^{+16}_{-15} geo-neutrino events, corresponding to $S(\mathrm{U+Th}) = 55^{+33}_{-31}$ TNU. From the median line of Figure 3, the radiogenic power is now:

$$H(\mathrm{U+Th}) = 36^{+35}_{-33}\mathrm{TW} \quad (\text{rate spectrum} + \text{new}^{13}\mathrm{C}(\alpha, \mathrm{n})^{16}\mathrm{O})$$

We also performed an analysis of the binned spectrum reported in Figure 3 of (Araki et al., 2005). This analysis gives $N(\mathrm{U+Th}) = 31^{+14}_{-13}$ counts, corresponding to $S(\mathrm{U+Th}) = 63^{+28}_{-25}$ TNU and thus:

$$H(\mathrm{U+Th}) = 44^{+31}_{-27}\mathrm{TW} \quad (\text{rate spectrum} + \text{new}^{13}\mathrm{C}(\alpha, \mathrm{n})^{16}\mathrm{O})$$

8. Future prospects

The present situation can be summarized in the following points:

- KamLAND has shown that the technique for exploiting geo-neutrinos in the investigation of the Earth's interior is now available.
- New data on $^{13}\mathrm{C}(\alpha, \mathrm{n})^{16}\mathrm{O}$ corroborate the evidence for geo-neutrinos in KamLAND data, which becomes close to 2.5σ.
- On the other hand, the determination of radiogenic heat power from geo-neutrino measurements is still affected by a 70% uncertainty. The best fit of $H(\mathrm{U+Th})$ is close to the prediction of maximal and fully radiogenic model, however the BSE prediction is within 1σ.
- The universal slope $dS/dH \sim 1$ TNU/TW means that for determining the radiogenic heat within ± 7 TW the experimental error has to be ± 7 TNU, i.e. factor four improvement with respect to present.

It looks to us that the following questions are relevant for the future:

- How shall we have definite (at least 3σ) evidence of geo-neutrinos?
- How much uranium and thorium are in the Earth's crust?
- How much in the mantle?
- What about the core?

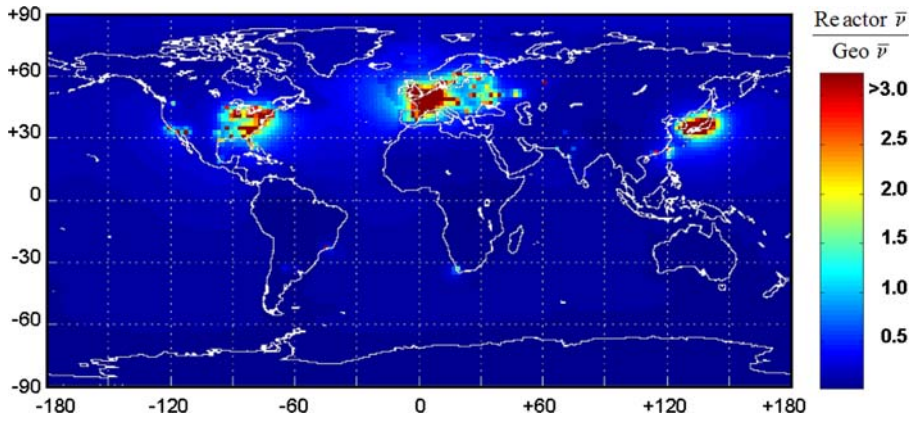

Figure 5. The ratio of reactor anti-neutrino events (in the geo-neutrino energy region) to the expected geo-neutrino events all over the globe.

A preliminary point for establishing suitable detector locations is the reactor background. Figure 5 shows the ratio of reactor events (in the geo-neutrino energy region) to the expected geo-neutrino events all over the globe. The location of KamLAND is obviously one of the worst for the study of geo-neutrinos.

The potential of different locations is summarized in Table VII, where we present the separate contributions to the geo-neutrino signal from crust and mantle according to our reference model, as well as the merit figure r = geo-neutrino events/reactor events.

With more statistics KamLAND should be capable of providing three sigma evidence of geo-neutrinos, but discrimination between BSE and fully radiogenic models definitely requires new detectors, with class and size

TABLE VII

The signal (U + Th) expected from the crust S_C, from the mantle S_M and the total signal S_{TOT} in Terrestrial Neutrino Units [TNU]

Location	S_C(U + Th)	S_M(U + Th)	S_{TOT}(U + Th)	r
Baksan	43.3	9.3	52.6	5.0
Hawaii	3.6	9.3	12.9	10.0
Homestake	43.8	9.3	53.1	5.0
Kamioka	26.4	9.3	35.7	0.1
Gran Sasso	32.8	9.3	42.1	1.1
Pyhasalmi	44.0	9.3	53.3	2.0
Sudbury	43.3	9.3	52.6	0.9
Curacao	24.3	9.3	33.6	10.0

The r factor is the ratio between the geo-neutrino events and reactor events. For this discussion, we use the asymptotic value of the survival probability $\langle P_{ee} \rangle = 0.59$.

similar to that of KamLAND, far away from nuclear power plants. Borexino should reach the 3σ evidence, but cannot go much further due to its relatively small size.

SNO^+ with liquid scintillator will have excellent opportunities to determine the uranium mass in the crust, which accounts for about 80% of the geo-neutrino signal at Sudbury. This will provide an important test of models for the Earth's crust.

A detector at Hawaii, very far from the continental crust and reactors, will be mainly sensitive to the mantle composition. We note that the amount of radioactive materials in this reservoir is the main uncertainty of geological models of the Earth. The expected signal, however, is rather small and this demands a several kilotons size.

For the very long term future, one can speculate about completely new detectors, capable of providing (moderately) directional information. These should allow identification of different geo-neutrino sources (crust, mantle and possibly core) in the Earth; in summary, ''se son rose fioriranno''.

Acknowledgments

We are grateful to C. Rolfs and his group for useful discussions and for allowing us to use their results. We thank for their useful comments A. Bottino, L. Carmignani, M. Contorti, E. Lisi, W. F. McDonough, K. Inoue, G. Ottonello, R. Raghavan, E. Sanshiro and R. Vannucci.

References

Anderson, D.: 2005, Energetics of the Earth and the Missing Heat Source Mystery, available at www.mantleplumes.org/Energetics.html.

Araki, T. *et al.*: 2005, (KamLAND coll.), *Nature* **436**, 499.

Araki, T. *et al.*: 2005, (KamLAND Collaboration), *Phys. Rev. Lett.* **94,** 081801 hep-ex/0406035.

Bair, J. K. and Haas, F. X.: 1973, *Phys. Rev.* **7**, 1356.

Bassin, C., Laske, G. and Masters, G.: 2000, *EOS Trans. Am. Geophys.* Union 81, F897 [http://mahi.ucsd.edu/Gabi/rem.html].

Condie, K. C.: 1993, *Chem. Geol.* **104**, 1.

Dziewonski, A. M. and Anderson, D. L.: 1981, *Earth Planet. Interact.* **25**, 297.

Fiorentini, G., Mantovani, F. and Ricci, B.: 2003a, *Phys. Lett. B* **557**, 139 [arXiv:nucl-ex/0212008].

Fiorentini, G., Lissia, M., Mantovani, F. and Vannucci, R.: 2003b, Astroparticle and high energy physics AHEP2003/035 [arXiv:hep-ph/0401085].

Fiorentini, G., Lissia, M., Mantovani, F. and Ricci, B.: 2003c, arXiv:physics/0305075.

Fiorentini, G., Lasserre, T., Lissia, M., Ricci, B. and Schönert, S.: 2003d, *Phys. Lett. B* **558**, 15 [arXiv:hep-ph/0301042].

Fiorentini, G., Lissia, M., Mantovani, F. and Ricci, B.: 2005a, *Phys. Lett. B* **629**, 77–82 hep-ph/0508048.
Fiorentini, G., Lissia, M., Mantovani, F. and Vannucci, R.: 2005b, *Phys. Rev. D* **72**, 03317 [arXiv:hep-ph/0501111].
Gao, S. et al.: 1998, *Geochimica et Cosmochimica Acta* **62**, 1959–1975.
GERM: 2003, The Geochemical Earth Reference Model, is available on the web at http://earthref.org.
Harissopulos, S. et al.: 2005, *Phys. Rev. C* **72**, 06281 [arXiv:nucl-ex/0509014].
Hofmann, A. W.: 1988, *Earth Planet Sci. Lett.* **90**, 297.
Hofmeister, A. M. and Criss, R. E.: 2005, *Tectonophysics* **395**, 159–177.
JENDL: 2005, Japanese Evaluated Nuclear Data Library, http://wwwndc.tokai.jaeri.go.jp/jendl/.
Jochum, K. P. et al.: 1986, *Nature* (London) **322**, 221.
Mantovani, F., Carmignani, L., Fiorentini, G. and Lissia, M.: 2004, *Phys. Rev. D* **69**, 013001 [arXiv:hep-ph/0309013].
McDonough, W. F.: 2003, in R. W. Carlson (ed.), *The Mantle and Core* Vol. 2, H. D. Holland and K. K. Turekian (eds.), *Treatise on Geochemistry*, Elsevier-Pergamon, Oxford, pp. 547–568.
O'Nions, R. K. and McKenzie, D.: 1993, *Philos. Trans. R. Soc. London A* **342**, 65.
Pollack, H. N., Hunter, S. J. and Johnson, J. R.: 1993, *Rev. Geophys.* **31**, 267–280.
Raghavan, R. S., Schönert, S., Enomoto, S., Shirai, J., Suekane, F., and Suzuki, A.: 1998, *Phys. Rev. Lett.* **80**, 635.
Rothschild, C. G., Chen, M. C. and Calaprice, F. P.: 1998, *Geophys. Res. Lett.* **25**, 1083 [arXiv:nucl-ex/9710001].
Rudnick, R. L. and Fountain, D. M.: 1995, *Rev. Geophys.* **33**, 267.
Shaw, D. M., Cramer, J. J., Higgins, M. D. and Truscott, M. G.: 1986, in J. Dawson *et al* (eds.), *The Nature of the Lower Continental Crust*, Geological Society of London, London, p. 275.
Taylor, S. R. and McLennan, S. M.: 1985. *The Continental Crust: its Composition and Evolution*, Blackwell Scientic, Oxford.
Togashi, S. *et al.*: 2000, *Geochem. Geophys. Geosyst. Electronic J. Earth Sci.* **1**, 2000GC00083.
Weaver, B. L. and Tarney, J.: 1984, *Nature (London)* **310**, 575.
Wedepohl, K. H.: 1995, *Geochim. Cosmochim. Acta* **59**, 1217.
White, W. M.: 1993, *Earth Planet Sci. Lett.* **115**, 211 [arXiv:hep-ph/0212202].
Zartman, R. E. and Haines, S.: 1988, *Geochim. Cosmochim. Acta* **52**, 1327.
Zhao, D., Horiuchi, S. and Hasegawa, A.: 1992, *Tectonophysics* **212**, 289–301.